ACS Medicinal Chemistry Letters

Letter

pubs.acs.org/acsmedchemlett

Structure-Based Design of Type II Inhibitors Applied to Maternal Embryonic Leucine Zipper Kinase

Christopher N. Johnson,*[,†] Christophe Adelinet,[§] Valerio Berdini,[†] Lijs Beke,[‡] Pascal Bonnet,[‡,∥] Dirk Brehmer,[‡] Frederick Calo,[†] Joseph E. Coyle,[†] Phillip J. Day,[†] Martyn Frederickson,[†] Eddy J. E. Freyne,[‡] Ron A. H. J. Gilissen,[‡] Christopher C. F. Hamlett,[†] Steven Howard,[†] Lieven Meerpoel,[‡] Laurence Mevellec,[§] Rachel McMenamin,[†] Elisabeth Pasquier,[§] Sahil Patel,[†] David C. Rees,[†] and Joannes T. M. Linders[‡]

[†]Astex Pharmaceuticals, 436 Cambridge Science Park, Milton Road, Cambridge CB4 0QA, United Kingdom

[‡]Janssen Research and Development, A Division of Janssen Pharmaceutica N.V., Turnhoutseweg 30, Beerse 2340, Belgium

[§]Janssen Research and Development, A Division of Janssen-Cilag , BP615-Chaussée du Vexin, 27106 Val-de-Reuil, France

Supporting Information

ABSTRACT: A novel Type II kinase inhibitor chemotype has been identified for maternal embryonic leucine zipper kinase (MELK) using structure-based ligand design. The strategy involved structural characterization of an induced DFG-out pocket by protein−ligand X-ray crystallography and incorporation of a slender linkage capable of bypassing a large gate-keeper residue, thus enabling design of molecules accessing both hinge and induced pocket regions. Optimization of an initial hit led to the identification of a low-nanomolar, cell-penetrant Type II inhibitor suitable for use as a chemical probe for MELK.

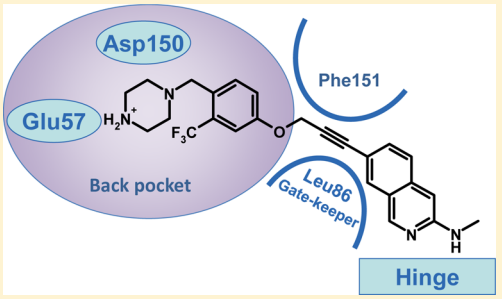

KEYWORDS: *Maternal embryonic leucine zipper kinase, fragment-based drug design, structure-based optimization*

Maternal embryonic leucine zipper kinase (MELK) has been suggested as a promising target for cancer treatment[1] with reports of increased MELK expression in multiple cancer types.[2−7] One challenge in assessing the biological role of MELK has been the lack of well-characterized selective inhibitors. For example, the MELK inhibitor OTSSP167 has shown promising activity in a number of phenotypic assays but no selectivity data is disclosed.[8] However, we recently reported the use of fragment-based drug design[9] (FBDD) to obtain MELK-T1 **1**, a selective chemical probe for MELK inhibition.[10] In this approach, a fragment binding to the hinge backbone was optimized by structure-guided design into a selective low nanomolar inhibitor. Protein−ligand X-ray crystallography of the MELK complex with **1** showed that the conserved Asp-Phe-Gly motif in the kinase activation loop adopted the so-called DFG-in conformation; MELK-T1 thus exemplifies a Type I inhibitor, albeit with an atypical trans-amide hinge binding motif. We were also interested in accessing Type II inhibitors, typified by a DFG-out conformation of the activation loop.

A number of design approaches to Type II inhibitors have been reported,[11] but for MELK, several challenges had to be overcome. Existing Type II chemotypes tend toward high molecular weight and lipophilicity because the molecules span a large distance between the hinge region and a back pocket beyond the gate-keeper residue characteristic of DFG-out structures. Our aim was to generate inhibitors with good ligand efficiency (LE),[12] suitable for use as chemical probes in cell-based assays and as starting points for efficient optimization into drug candidates. A second challenge was the large size of the gate-keeper (GK) residue for MELK, namely, Leu86. For a putative molecule binding to both hinge and back pocket, a large GK provides a steric barrier for any linkage, so affording a significant design challenge. Typical Type II inhibitors present an amide or urea linker in the region between the hinge and back pocket; accommodation of such groups is more challenging with a large GK. However, we were encouraged that Type II structures are precedented for c-Met, where the GK is also leucine.[13] Another potential difficulty was obtaining high quality structural information on a DFG-out form of MELK. To support the FBDD campaign that led to **1**, soakable crystal forms of MELK were developed in which the protein adopted the DFG-in conformation. All X-ray validated hits from the MELK fragment screen bound to this conformation; hence the fragment screen, per se, did not provide useful Type II starting points. We anticipated a challenge for identification of Type II ligands by crystal soaking experiments using a Type I

Special Issue: New Frontiers in Kinases

Received: March 28, 2014
Accepted: May 15, 2014
Published: May 23, 2014

   dx.doi.org/10.1021/ml5001273 | *ACS Med. Chem. Lett.* 2015, 6, 31−36

conformation of MELK, as this would involve significant protein movement.[14] Such a conformational change could incur a large energy penalty and might be incompatible with the crystal forms available.

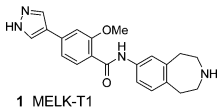

1 MELK-T1
MELK IC_{50} 37 nM (LE 0.38)

This letter describes structure-based design of a novel kinase Type II inhibitor chemotype, realization of which involved integration of three key design elements: (i) a moiety capable of binding in a putative back pocket; (ii) a linker capable of bypassing the large leucine GK; and (iii) a ligand-efficient hinge binding motif providing an appropriate growth vector to allow linker attachment with minimum disruption of geometry (Figure 1).

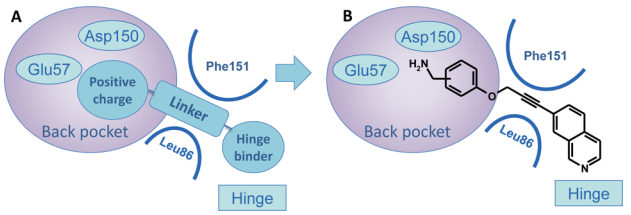

Figure 1. Design strategy for Type II MELK inhibitors. (A) Schematic showing the three design elements with MELK binding site for context. (B) Set of compounds targeted for synthesis.

Of the three key design elements, element (i) represented a major challenge since no structural information was initially available concerning the putative back pocket and the side chain residues lining it. Although fragment screening failed to generate any MELK DFG-out conformations, a partial breakthrough occurred when follow-up screening was carried out on a subset of hits. It was found that a number of lipophilic primary aryl-alkylamines induced a flip of the DFG motif and that electron density was evident in the putative back pocket consistent with ligand binding, though data quality was suboptimal. A common feature of these structures was formation of salt bridges between the charged amine of the ligand with acidic residues Glu57 (situated on the α-C helix) and/or Asp150 (from the DFG motif). Direct optimization of these low potency molecules ($IC_{50} \geq 100\ \mu M$) was unsuccessful, a contributing factor being the low quality of structural data, but the observations provided a vital clue for design of back pocket binding motifs, in particular the need for a cationic center. Importantly, the data provided reassurance that Type II conformations were accessible in practice for MELK, explicitly in the crystal forms developed for fragment screening.

The next element considered was the linker; this should function as a suitable spacer while providing an exit from the back pocket compatible with steric constraints at the point of entry into the hinge binding region. Such constraints were apparent from examination of our Type II structures, where a narrow connecting tunnel was observed, the primary steric restrictions being provided by Leu86 and the DFG phenylalanine (Phe151). An alkyne-containing linker was therefore chosen by virtue of having low steric demand; this group precisely defined a vector for linking to a hinge binding element. The primary selection criterion for the latter was the closeness of match between the alkyne vector and the growth vectors provided by candidate hinge binding elements. We performed an alignment of MELK with all PDB and Astex-proprietary liganded kinase structures, then selected hinge binding motifs satisfying appropriate angular and distance constraints; from these, 7-isoquinolinyl was chosen for an initial study. Having now considered all three design elements (Figure 1A), we designed a targeted set of compounds (Figure 1B) and were gratified to find a hit **2** (IC_{50} 24 μM, LE 0.29; Table 1 and Scheme 2), which served as a starting point for optimization.

Table 1. MELK Inhibitory Activity of Compounds 2−9

Cpd	Structure	MELK IC_{50} (μM)[a] Astex	LE[b]	MELK IC_{50} (μM)[a] Millipore	LE[b]
2	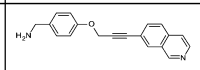	24	0.29	NT	
3	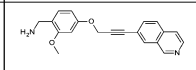	5.1	0.31	NT	
4	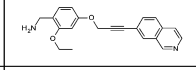	0.65	0.34	NT	
5	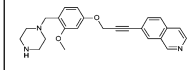	0.72	0.29	0.52	0.30
6	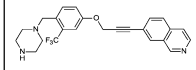	0.30	0.29	0.076	0.32
7	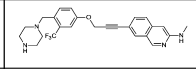	NT		0.019	0.32
8	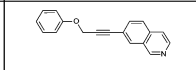	52% @ 300 μM	0.24[c]	NT	
9	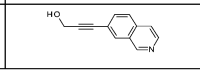	3.1	0.54	NT	

[a]Assay conditions described in Supporting Information. [b]LE = ligand efficiency = $-RT\ \ln(IC_{50})/HAC$ where HAC = heavy atom count. [c]On the basis of an estimated IC_{50} value of 300 μM.

Compounds **2**−**7** (Table 1) were prepared as illustrated in Schemes 1 and 2 (for experimental details and compound characterization of compounds **2**−**9**, see Supporting Information).

A key step in the synthesis of all compounds was C−C bond formation to a terminal alkyne using a Sonagashira coupling with an isoquinoline (IQ) bearing a leaving group at C-7 and further substituted as appropriate. For compounds **2**−**6**, 7-trifluoromethylsulfonyloxy-isoquinoline[15] was the coupling partner, while **7** required preparation of disubstituted IQ **12**

Scheme 1. Preparation of Intermediate 12[a]

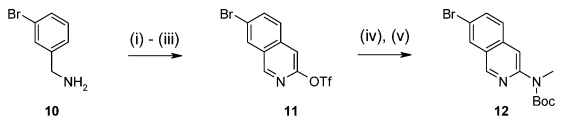

10 **11** **12**

[a]Reagents and conditions: (i) $(EtO)_2CHCO_2Et$, DIPEA, 130 °C; (ii) H_2SO_4, RT; (iii) 1. $(CF_3SO_2)_2O$, pyridine, RT. 2. Chromatographic separation (SiO_2); (iv) CH_3NH_2, THF, autoclave, 100 °C; (v) $(Boc)_2O$, NaHDMS, THF, 5 °C to RT. For yields, see experimental procedures in Supporting Information.

dx.doi.org/10.1021/ml5001273 | ACS Med. Chem. Lett. 2015, 6, 31−36

Scheme 2. Preparation of Compounds 2−7[a]

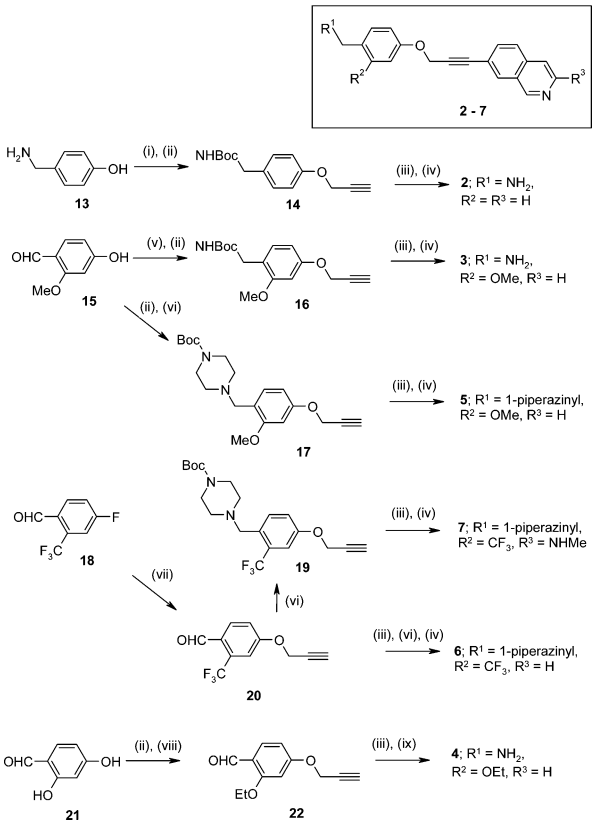

[a]Reagents and conditions: (i) $(Boc)_2O$, NaOH, H_2O, THF, RT; (ii) 3-bromo-1-propyne, K_2CO_3, MeCN or acetone or 2-butanone, RT or reflux; (iii) 7-trifluoromethylsulfonyloxy-isoquinoline (for **2**−**6**) or **12** (for **7**), $Pd(PPh_3)_4$, CuI, Et_3N, DMF, microwave at 100 °C or RT; (iv) HCl, 1,4-dioxane, EtOAc, RT; (v) $BocNH_2$, TFA, Et_3SiH, CH_2Cl_2, MeCN, RT; (vi) 1-Boc-piperazine, $NaBH(OAc)_3$, CH_2ClCH_2Cl, RT; (vii) 2-prop-2-yn-1-ol, K_2CO_3, MeCN, reflux; (viii) EtI, K_2CO_3, 2-butanone, 55 °C; (ix) NH_4OAc, $NaBH_3CN$, MeOH, RT. For yields, see experimental procedures in Supporting Information.

(Scheme 1). Acylation of 3-bromobenzylamine **10** was followed by acid-mediated cyclization to give a 3:2 mixture of regioisomers. Following reaction with trifluoromethyl-sulfonic anhydride, the resulting mixture of triflates was separated by chromatography to give **11**. Reaction with methylamine was then carried out, and this was followed by Boc protection to give **12**.

Several approaches were successfully employed to provide the required terminal alkyne coupling partners (Scheme 2). Protection of 4-hydroxybenzylamine **13** and alkylation with 3-bromo-1-propyne gave **14**. Reductive amination of aldehyde **15** with *tert*-butyl carbamate and subsequent propynylation gave coupling partner **16**. The same aldehyde also provided compound **17** using a similar sequence. For trifluoromethyl substituted compounds such as **19** and **22**, the propynyloxy group was introduced by nucleophilic substitution to give **20**. Reductive amination as before gave **19**, and this was coupled with **12** to give MELK-T2 **7**. The aldehyde group in **20** proved to be compatible with the coupling conditions, allowing introduction of the protected piperazine side chain as the penultimate step, whereupon acid-mediated deprotection afforded compound **6**. This same approach was used for compound **4**, starting from 2,4-dihydroxybenzaldehyde **21**, where two successive alkylations gave **22**. Coupling of **22** proceeded in excellent yield (81%), and this was followed by reductive amination to give **4**. Compounds **8** and **9** were prepared in an analogous manner by Sonagashira coupling of 7-trifluoromethyl-sulfonyloxyisoquinoline with 3-phenoxy-1-propyne and 3-trimethylsilyloxy-1-propyne, respectively. In the case of **9**, the intermediate trimethylsilyl derivative was not isolated due to deprotection upon work-up. Compounds of Table 1 were assessed for inhibition of MELK kinase activity using a radioactive filter binding assay (see Supporting Information).

Although **2** had measurable potency and moderate LE, it was not possible to obtain a crystal structure to confirm a Type II binding mode. However, a focused compound set based around **2** resulted in identification of compounds **3** and **4** with improved potency and LE > 0.3. An X-ray crystal structure was solved for **4** (Figure 2), demonstrating proof-of-principle for

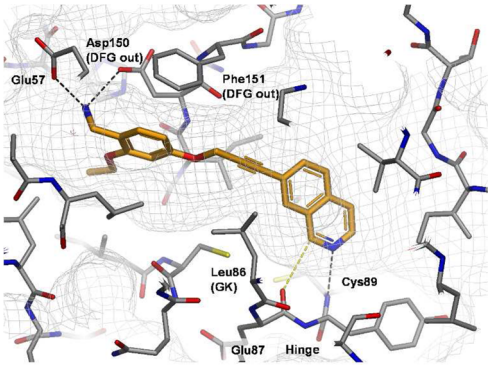

Figure 2. X-ray crystal structure of **4** bound to MELK (DFG-out conformation) showing protein surface as gray mesh and key hydrogen bonds and salt bridges as dotted lines.

the design strategy, with the protein in a DFG-out conformation. The primary amine in **4** forms salt bridges with Glu57 and Asp150, while the attached substituted phenyl group occupies a lipophilic pocket, forming an edge-to-face interaction with Phe151. The alkyne terminal vector is sufficiently well-aligned to position the IQ ring system for hinge interactions: the IQ nitrogen acts as an acceptor for the NH of Cys89, and a C−H hydrogen bond is formed between the IQ C-1 hydrogen and backbone carbonyl of Glu87, while the planar IQ bicycle packs efficiently into the adenine binding pocket. A number of atypical features are apparent in this structure, both in terms of protein−ligand interactions and kinase conformation. Type II kinase inhibitors typically possess linkers capable of forming hydrogen bonds with residues at the entrance to the back pocket such as the catalytic lysine or α-C helix glutamate. In contrast, **4** is atypical in that the ethynylmethoxy linker makes no polar interactions; instead, the alkyne performs the essential function of traversing a narrow tunnel in the region of Leu86. Comparison of protein conformations seen in the costructures of **1** (Type I) and **4** (Type II) shows an expected difference in the position of the DFG motif (Figure 3), but there is, in addition, a major difference in the position of Glu57: in the Type I structure, a canonical salt bridge is formed with catalytic Lys40, whereas in the Type II structure the Glu57 side chain is directed into the back pocket accompanied by an α-C helix rotation. Such a large movement of the α-C helix is also atypical, and the presence of

dx.doi.org/10.1021/ml5001273 | ACS Med. Chem. Lett. 2015, 6, 31−36

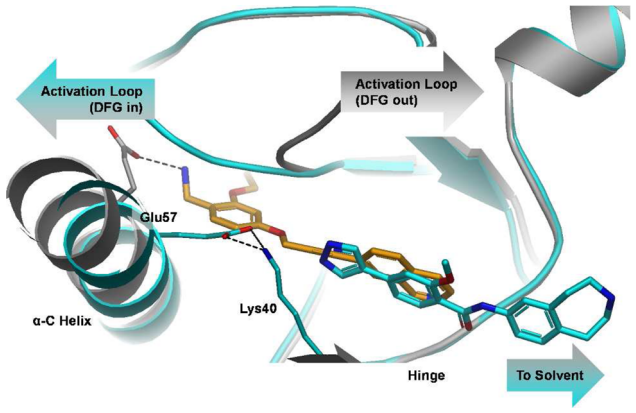

Figure 3. Overlay of X-ray crystal structures of **1** (light blue) and **4** (orange) bound to MELK. The DFG-in conformation, which binds **1**, is shown in cyan, while the DFG-out conformation, which binds **4**, is shown in gray. Salt bridges formed by Glu57 are shown as dotted lines.

a ligand cationic center is likely to be the driver for both conformational changes observed.

Following this breakthrough, **3** and **4** provided a starting point for further optimization, namely, variation of the aliphatic amine side chain and alternative substitutions on both phenyl spacer and IQ moiety. Replacement of NH_2 with piperazinyl **5** (IC_{50} 0.72 μM, LE 0.29) gave a 7-fold potency increase compared to **3**. The binding mode (Figure 4) was similar to **4**

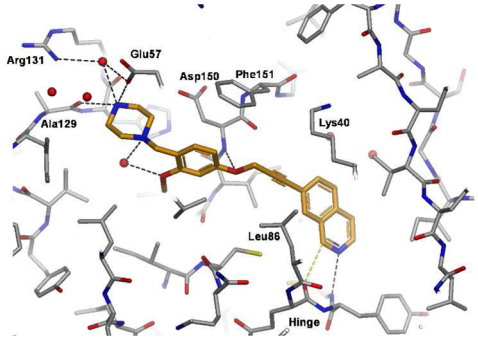

Figure 4. X-ray crystal structure of compound **5** bound to MELK (DFG-out conformation) showing key hydrogen bonds and salt bridges as dotted lines and water molecules as red spheres.

with the exception of polar interactions made in the back pocket. The protonated piperazine forms a salt bridge with Glu57 and donates hydrogen bonds to the backbone carbonyl of Ala129 and to a water molecule bound to His130 and Arg131. Unlike the costructure with **4**, Asp150 makes no productive interaction with the ligand; there is apparent flexibility as to the nature of the basic group that can be accommodated in the back pocket.

Replacement of the alkoxy substituent was investigated; here, trifluoromethyl **6** gave a further 2-fold increase in potency. The crystal structure of **5** showed that there was an opportunity to donate an additional hydrogen bond to the hinge via the backbone carbonyl of Cys89, leading to methylamino derivative **7** (IC_{50} 0.019 μM, LE 0.32; Millipore assay). In the Millipore assay **6** had IC_{50} 0.076 μM and LE 0.32; hence, the addition of the methylamino group resulted in 4-fold increased potency for **7**. Compound **7** was screened against a panel of 243 kinases and showed >50% inhibition at 1 μM against only 31 enzymes (most potent shown in Table 2). Interestingly, significant

Table 2. Selectivity Profile of 7 (MELK-T2)

kinase[a]	% inh @ 1 μM	IC_{50} (nM)
MELK	100	20
Flt-1	98	20
RET	98	10
Flt-4	98	30
NTKR2	95	190
CSF1R	94	46
Yes-1	94	30
DDR2	93	290
Flt-3	92	50
FGFR1	91	250

[a]Millipore kinase screening panel; for details, see Supporting Information. Compound **7** gave >50% inhibition at 1 μM for 31/243 kinases screened; only most potent interactions shown.

activity was found against Flt3 (55 nM), as previously seen for MELK-T1 **1**. Given a lack of Flt3 structural information, it is not possible to pass comment on the likely binding mode (Type II vs Type I) for **7** in Flt3, although the DFG-out conformation is precedented for this kinase,[16] and interestingly, it possesses a Phe GK residue. Off-target activity at Flt3 afforded an opportunity to assess intracellular activity for **7**, as was previously determined for **1**.[10] In an engineered Ba/F3 Flt3-dependent cell assay[17] **7** showed potent inhibitory activity, with IC_{50} 44 nM. Hence compound **7** is cell penetrant and should therefore be useful as chemical probe for elucidating cell phenotypic effects resulting from MELK inhibition.

Concomitantly with the optimization of **2** to give **7**, we probed the importance of individual ligand structural elements for inducing MELK conformational changes. When the aminomethyl group from compound **2** was removed to give phenoxy **8**, a dramatic loss of potency and LE was observed. Unfortunately we were unable to obtain a crystal structure of **8** bound to MELK and hence ascertain protein conformation. Modeling suggested that it was unlikely for **8** to bind to the Type I conformation (as defined by the complex with **1**) and at the same time maintain the binding pose at the hinge shown for **2** in Figure 2. One possible interpretation is that MELK adopts the Type II conformation with **2**, and significant potency is derived from the salt bridge interactions in the back pocket. Alternatively, the protein may adopt the Type I conformation, and the ligand flips orientation at the hinge so that the substituted alkyne is directed toward the solvent exposed region.

Further deconstruction of **2** by removal of the entire back pocket binding motif gave primary alcohol **9**, with a remarkable increase in potency and LE. The crystal structure (Figure 5) gave an explanation for this discontinuity; while orientation and backbone interactions of the hinge binding element are the same as those of **2**, the protein is now DFG-in. The OH forms multiple hydrogen bonds, e.g., with the Glu57 side chain and backbone NH of Asp150. The large increase in LE for this Type I inhibitor vs compounds **2**–**7** may reflect the energy penalty incurred for the switch in protein conformation to the Type II form.

In conclusion, we have described a novel alkyne Type II kinase inhibitor chemotype and a design strategy with potential application to other kinase enzymes possessing a leucine GK. The Bcr-Abl inhibitor ponatinib[18] also possesses an alkyne linker but, in contrast to inhibitors described above, forms hydrogen bond interactions to the protein at the entrance to

dx.doi.org/10.1021/ml5001273 | ACS Med. Chem. Lett. 2015, 6, 31–36

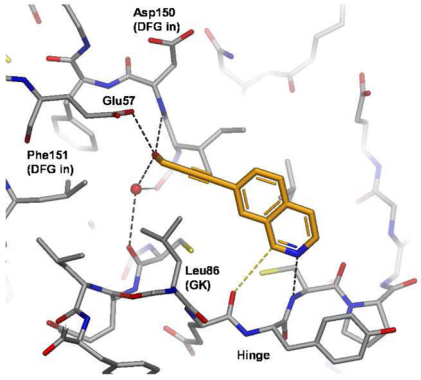

Figure 5. X-ray crystal structure of **9** bound to MELK (DFG-in conformation) showing key hydrogen bonds as dotted lines and a water molecule as a red sphere.

the back pocket. Our strategy relied on observation by protein X-ray crystallography of back pocket binding events in an induced Type II conformation. Although initial structural data were of poor quality, enough information was provided to generate a hypothesis, enabling the design of a back pocket binding motif (i) and an appropriately attached linker (ii) capable of bypassing the large gate-keeper residue, then selection of an appropriate hinge binding element (iii) with suitable alignment vectors. Deconstruction of initial hit molecules showed that all three elements were required for potent Type II inhibition; notably removal of the back pocket motif resulted in a Type I inhibitor. Once higher quality structural data were available, initial hits were efficiently optimized into MELK-T2 **7**, a low nanomolar inhibitor. MELK-T2 showed evidence for intracellular kinase inhibitory activity so, like MELK-T1 **1**, has potential as a MELK inhibitor chemical probe as well as a starting point for further optimization.

■ ASSOCIATED CONTENT

Supporting Information

Assay conditions; experimental procedures and characterization data for novel compounds and intermediates; crystallographic details. This material is available free of charge via the Internet at http://pubs.acs.org.

■ AUTHOR INFORMATION

Corresponding Author

*(C.N.J.) Tel: 44-1223-226220. Fax: 44-1223-226201. E-mail: Chris.Johnson@astx.com.

Present Address

‖(P.B.) Institut de Chimie Organique et Analytique (ICOA), Université d'Orléans, UMR CNRS 7311, 45057 Orléans Cedex 2, France.

Notes

The authors declare no competing financial interest.

■ ACKNOWLEDGMENTS

We would like to thank Prof. Jan Cools (Catholic University Leuven, Leuven, Belgium) for the gift of the Ba/F3 Flt3 cell line.

■ REFERENCES

(1) Gray, D.; Jubb, A. M.; Hogue, D.; Dowd, P.; Kljavin, N.; Yi, S.; Bai, W.; Frantz, G.; Zhang, Z.; Koeppen, H.; de Sauvage, F. J.; Davis, D. P. Maternal embryonic leucine zipper kinase/murine protein serine-threonine kinase 38 is a promising therapeutic target for multiple cancers. *Cancer Res.* **2005**, *65*, 9751−9761.

(2) Nakano, I.; Masterman-Smith, M.; Saigusa, K.; Paucar, A. A.; Horvath, S.; Shoemaker, L.; Watanabe, M.; Negro, A.; Bajpai, R.; Howes, A.; Lelievre, V.; Waschek, J. A.; Lazareff, J. A.; Freije, W. A.; Liau, L. M.; Gilbertson, R. J.; Cloughesy, T. F.; Geschwind, D. H.; Nelson, S. F.; Mischel, P. S.; Terskikh, A. V.; Kornblum, H. I. Maternal embryonic leucine zipper kinase is a key regulator of the proliferation of malignant brain tumors, including brain tumor stem cells. *J. Neurosci. Res.* **2008**, *86*, 48−60.

(3) Pickard, M. R.; Green, A. R.; Ellis, I. O.; Caldas, C.; Hedge, V. L.; Mourtada-Maarabouni, M.; Williams, G. T. Dysregulated expression of Fau and MELK is associated with poor prognosis in breast cancer. *Breast Cancer Res.* **2009**, *11*, R60.

(4) Lin, M.-L.; Park, J.-H.; Toshihiko Nishidate, T.; Nakamura, Y.; Katagiri, T. Involvement of maternal embryonic leucine zipper kinase (MELK) in mammary carcinogenesis through interaction with Bcl-G, a pro-apoptotic member of the Bcl-2 family. *Breast Cancer Res.* **2009**, *11*, R17.

(5) Kuner, R.; Fälth, M.; Pressinotti, N. C.; Brase, J. C.; Puig, S. B.; Metzger, J.; Gade, S.; Schäfer, G.; Bartsch, G.; Steiner, E.; Klocker, H.; Sültmann, H. The maternal embryonic leucine zipper kinase (MELK) is upregulated in high-grade prostate cancer. *J. Mol. Med.* **2013**, *91*, 237−248.

(6) Ryu, B.; Kim, D. S.; DeLuca, A. M.; Alani, R. M. Comprehensive expression profiling of tumor cell lines identifies molecular signatures of melanoma progression. *PLoS One* **2007**, *2*, e594.

(7) Ku, J.-L.; Shin, Y.-K.; Kim, D.-W.; Kim, K.-H.; Choi, J.-S.; Hong, S.-H.; Jeon, Y.-K.; Kim, S.-H.; Kim, H.-S.; Park, J.-H.; Kim, I.-J.; Park, J.-G. Establishment and characterization of 13 human colorectal carcinoma cell lines: mutations of genes and expressions of drug-sensitivity genes and cancer stem cell markers. *Carcinogenesis* **2010**, *31*, 1003−1009.

(8) Chung, S.; Suzuki, H.; Miyamoto, T.; Takamatsu, N.; Tatsuguchi, A.; Ueda, K.; Kijima, K.; Nakamura, Y.; Matsuo, Y. Development of an orally-administrative MELK-targeting inhibitor that suppresses the growth of various types of human cancer. *Oncotarget* **2012**, *3*, 1629−1640.

(9) Jhoti, H.; Williams, G.; Rees, D. C.; Murray, C. W. The 'rule of three' for fragment-based drug discovery: where are we now? *Nat. Rev. Drug Discovery* **2013**, *12*, 644−645.

(10) Johnson, C. N.; Berdini, V.; Beke, L.; Bonnet, P.; Brehmer, D.; Coyle, J. E.; Day, P. J.; Frederickson, M.; Freyne, E. J. E.; Gilissen, R. A. H. J.; Hamlett, C. C. F.; Howard, S.; Meerpoel, L.; McMenamin, R.; Patel, S.; Rees, D. C.; Sharff, A.; Sommen, F.; Wu, T.; Linders, J. T. M. Fragment-Based Discovery of Selective Type I Inhibitors of Maternal Embryonic Leucine Zipper Kinase. *ACS Med. Chem. Lett.* **2014**, DOI: 10.1021/ml5001245.

(11) Blanc, J.; Geney, R.; Menet, C. Type II Kinase Inhibitors: An Opportunity in Cancer for Rational Design. *Anti-Cancer Agents Med. Chem.* **2013**, *13*, 731−747.

(12) LE = $-\Delta G/\mathrm{HAC} \approx -RT \ln(\mathrm{IC}_{50})/\mathrm{HAC}$. Hopkins, A. L.; Groom, C. R.; Alex, A. Ligand efficiency: a useful metric for lead selection. *Drug Discovery Today* **2004**, *9*, 430−431.

(13) Schroeder, G. M.; Chen, X. T.; Williams, D. K.; Nirschl, D. S.; Cai, Z. W.; Wei, D.; Tokarski, J. S.; An, Y.; Sack, J.; Chen, Z.; Huynh, T.; Vaccaro, W.; Poss, M.; Wautlet, B.; Gullo-Brown, J.; Kellar, K.; Manne, V.; Hunt, J. T.; Wong, T. W.; Lombardo, L. J.; Fargnoli, J.; Borzilleri, R. M. Identification of pyrrolo[2,1-f][1,2,4]triazine-based inhibitors of Met kinase. *Bioorg. Med. Chem. Lett.* **2008**, *18*, 1945−1951.

(14) Murray, C. W.; Verdonk, M. L.; Rees, D. C. Experiences in fragment-based drug discovery. *Trends Pharmacol. Sci.* **2012**, *33*, 224−232.

(15) Nilson, M. G.; Funk, R. L. Total synthesis of (±)-cortistatin J from furan. *J. Am. Chem. Soc.* **2011**, *133*, 12451−12453.

(16) Griffith, J.; Black, J.; Faerman, C.; Swenson, L.; Wynn, M.; Lu, F.; Lippke, J.; Saxena, K. The structural basis for autoinhibition of FLT3 by the juxtamembrane domain. *Mol. Cell* **2004**, *13*, 169−178.
(17) Warmuth, M.; Kim, S.; Gu, X.-J.; Xia, G.; Adrián, F. Ba/F3 cells and their use in kinase drug discovery. *Curr. Opin. Oncol.* **2007**, *19*, 55−60.
(18) O'Hare, T.; Shakespeare, W. C.; Zhu, X.; Eide, C. A.; Rivera, V. M.; Wang, F.; Adrian, L. T.; Zhou, T.; Huang, W. S.; Xu, Q.; Metcalf, C. A.; Tyner, J. W.; Loriaux, M. M.; Corbin, A. S.; Wardwell, S.; Ning, Y.; Keats, J. A.; Wang, Y.; Sundaramoorthi, R.; Thomas, M.; Zhou, D.; Snodgrass, J.; Commodore, L.; Sawyer, T. K.; Dalgarno, D. C.; Deininger, M. W.; Druker, B. J.; Clackson, T. AP24534, a pan-BCR-ABL inhibitor for chronic myeloid leukemia, potently inhibits the T315I mutant and overcomes mutation-based resistance. *Cancer Cell* **2009**, *16*, 401−412.